Journal of Applied Phycology (2018) 30:2259–2271
https://doi.org/10.1007/s10811-018-1477-3

Elucidating the role of nutrients in C-phycocyanin production by the halophilic cyanobacterium *Euhalothece* sp.

Trisha Mogany[1] · Feroz Mahomed Swalaha[2] · Sheena Kumari[1] · Faizal Bux[1]

Received: 4 October 2017 / Revised and accepted: 9 April 2018 / Published online: 16 May 2018

Abstract

In this study, a novel halophilic cyanobacterium was isolated and identified as *Euhalothece* sp. KZN. This fast-growing strain had the ability to synthesise high yields (12 mg g^{-1}) of C-phycocyanin (C-PC), a highly fluorescent blue light-harvesting pigment with numerous potential uses in the biotechnology and commercial sectors. This study elucidated the individual and interactive role of different nutrients in BG11 growth medium for enhancing C-PC production in *Euhalothece* sp. KZN. Nine components of BG11 medium were screened for their effects via fractional factorial design (FFD). The results revealed a significant influence of nutrients, viz. $MgSO_4$, $NaNO_3$ and minor nutrients (citric acid, EDTA-iron citrate, $CaCl_2$ and Na_2CO_3) on C-PC yield. These three components were further explored for their optimum concentration for enhancing C-PC production using a central composite design. The optimum values for these essential nutrients were found to be as follows: 0.10 g L^{-1} of $MgSO_4$, 1.67 g L^{-1} of $NaNO_3$ and 10 mL L^{-1} of minor nutrients which resulted in a 280% increase in C-PC yield with predicted and actual values of 43.97 and 45 mg g^{-1}, respectively. *Euhalothece* sp. KZN is a strong potential candidate for C-PC production and can be further exploited to produce this industrially valuable compound.

Keywords *Euhalothece* sp. · Cyanobacteria · C-phycocyanin · Pigment · Nutrients · Design of experiments

Introduction

The genus *Euhalothece* comprises unicellular, marine cyanobacteria that are morphologically diverse and ecologically versatile (Bandyopadhyay et al. 2011). This oxygenic photosynthetic group of microorganisms is highly adaptable to varying light conditions due to the presence of large antenna complexes called phycobilisomes (PBSs) in photosystem I which can absorb and transfer light of different wavelengths (500–650 nm range) to photosynthetic reaction centres (Prasanna et al. 2004). These PBSs are composed of pigmented phycobiliproteins (PBPs) and colourless linker polypeptides (Glazer 1994; Sun et al. 2009a). The PBS has a core made up of allophycocyanin (C-APC) with rods of C-phycocyanin (C-PC), and sometimes phycoerythrin (C-PE) or phycoerythrocyanin (C-PEC) (Singh et al. 2012). Each subunit of PBP contains one or more chromophores, phycourobilin (PUB), phycoviolobilin (PVB), phycoerythrobilin (PEB) and phycocyanobilin (PCB) linked to specific cysteines in apoprotein by thioether bonds (Eriksen 2008). C-phycocyanin exists as a trimer from the aggregation of three alpha and beta ($\alpha\beta$) monomers, with a molecular weight of ± 232 kDa (Patel et al. 2005), absorption of 620 nm and emission maxima of 640 nm (Kuddus et al. 2013).

C-PC and related PBPs have shown great commercial potential with applications in the pharmaceutical, nutraceutical, food and cosmetic industries, as well as in clinical diagnostics and biomedical research (Manirafasha et al. 2016). Although the market size for C-PC applications has not being accurately established, a market analysis indicated that in 2016, the food colourant market reached US$13 billion with approximately 6.5% growth rate per year (Kannaujiya et al. 2017). The market for the nutraceutical segment of food industry for C-PC is estimated at between US$6 billion and US$60 billion (Rodríguez-Sánchez et al. 2012; Leu et al. 2013; Johnson et al. 2014). The commercial value of C-PC is directly related to its purity ratio (A_{620}/A_{280}), varying from US$3 to

Electronic supplementary material The online version of this article (https://doi.org/10.1007/s10811-018-1477-3) contains supplementary material, which is available to authorized users.

✉ Faizal Bux
faizalb@dut.ac.za

[1] Institute for Water and Wastewater Technology, Durban University of Technology, Durban 4001, South Africa

[2] Department of Biotechnology and Food Technology, Durban University of Technology, Durban 4001, South Africa

US$25 mg^{-1} for food and cosmetic grade pigments, whereas highly purified reactive grade molecules can be sold for up to US$1500 mg^{-1}. However, the successful application and production of C-PC depend on the nature of the organism, its growth characteristics, ability to scale up and, most importantly, accumulation and yield of C-PC (Eriksen 2008; Sekar and Chandramohan 2008; Kaushal et al. 2017).

The first steps in biosynthesis of PBP in cyanobacteria are the transcription and translation of amino acids, proteins and phycobilins, following the ligation of phycobilins to apoproteins with the aid of enzyme, lyases to form the C-PC (Wiethaus et al. 2010). Nutrients stimulate the production of PBPs by inducing the biosynthetic enzymes or by increasing the amount of heme and biliverdin (BV) precursors (Manirafasha et al. 2016). Nitrogen (N) is the major nutrient that is primarily used for cell growth, biomass production and protein and tetrapyrrole synthesis (Chaneva et al. 2007). Whereas, secondary nutrients, such as magnesium (Mg), and minor nutrients, which include iron (Fe), mainly serve as cofactors or prosthetic groups by forming a bridge between the biosynthetic enzymes and a substrate. There are some studies that report nutrient optimisation for C-PC production. For example, Johnson et al. (2014) found that when *Nostoc* sp. was grown in 1.5 g L^{-1} of $NaNO_3$ and 0.8 g L^{-1} of Na_2CO_3, a maximum C-PC yield of 42 mg g^{-1} was achieved. Pandey and Pandey (2008) reported that C-PC production in *Nostochopsis lobatus* was increased up to 58.72 mg g^{-1} when the BG11 growth medium was supplemented with 10 mg L^{-1} of K_2HPO_4 and 3 mg L^{-1} of $FeNH_4$ citrate. In another study, *Geitlerinema sulphureum* grown in Zarrouk's medium supplemented with 3.5 g L^{-1} of $NaNO_3$ and 6.24 g L^{-1} of Na_2CO_3 achieved 71 mg mL^{-1} of C-PC (Kenekar and Deodhar 2013). Very few studies have used response surface methodology (RSM) to enhance the C-PC production in cyanobacteria. Hong and Lee (2008) used a central composite design to optimise the culture media and reported that *Synechocystis* sp. produced 25.9 mg mL^{-1} when grown in 0.88 g L^{-1} $NaNO_3$ and 0.32 g L^{-1} K_2HPO_4. Similarly, using RSM, Deshmukh and Puranik (2012) reported 23 mg L^{-1} C-PC yield when *Synechocystis* sp. was cultivated in 0.052 g L^{-1} $CaCl_2{\cdot}2H_2O$ and 0.10 g L^{-1} Na_2CO_3. To date, there has been limited research outlining the effect of these nutrients on major biosynthetic enzymes involved in the regulation and accumulation of C-PC in cyanobacteria. The focus of this study was to (1) enhance C-PC yield in *Euhalothece* sp. KZN, (2) evaluate the role of essential nutrients in C-PC production and (3) gain insights on interactions amongst the nutrients. This was performed by screening and optimisation of BG11 medium components via fractional factorial design (FFD) and RSM, respectively. To our knowledge, this is the first study that explained the role of these optimised nutrients in the C-PC biosynthesis while enhancing the C-PC yield in the *Euhalothece* sp. KZN.

Materials and methods

Cyanobacterium isolation

The cyanobacterium was isolated from a hypersaline environment (St. Lucia Estuary, KwaZulu-Natal, South Africa; 27.976 S, 32.362 E). The physiochemical parameters such as temperature (30 °C), pH (8.0), dissolved oxygen (9.3 mg L^{-1}) and salinity (120 g L^{-1}) of the water samples were measured during the time of sample collection using a multiparameter YSI 556 MPS system (Yellow Spring Systems, USA). Isolation and purification of the cyanobacterium was carried out by continuous streak plating on 1% agar BG11 medium (pH 7.0) (Allen and Stanier 1968; Rippka et al. 1979; Waterbury and Stanier 1981). Obtained single colonies were inoculated into BG11 broth medium and incubated under the following cultivation conditions: Sylvania Grolux T8 illumination of 80 μmol photons m^{-2} s^{-1}, for 16-h light/8-h dark cycles at 29 ± 2 °C for 3 weeks. Wet mounts were performed using light microscopy (Nikon Eclipse 80*i* phase contrast, Japan) to ensure purity of the culture and observe morphological features. The isolate was identified to genus level on the basis on the proposed classification by Komárek (2016).

Partial 16S ribosomal RNA gene sequencing and analysis

Genomic DNA was extracted from exponentially grown cyanobacterial culture in BG11 medium using the FastDNA SPIN Kit for Soil (Mo Bio, USA) according to the manufacturer's instruction. The partial 16S ribosomal ribonucleic acid (rRNA) gene amplification was done using cyanobacteria-specific primers CYA106F (5′CGG ACG GGT GAG TAA CGC GTG A3′) and CYA781R (5′GAC TAC TGG GGT ATC TAA TCC CAT T3′) according to Nübel et al. (1997) in a Verity 96 well thermal cycler (Applied Biosystems, USA). The PCR conditions optimised include the following: initial denaturation at 94 °C for 3 min, followed by 35 cycles of denaturation at 94 °C for 1 min; primer annealing at 59 °C for 1.5 min; and extension at 72 °C for 2 min, followed by a final extension at 72 °C for 5 min. The amplified products were confirmed using gel electrophoresis and thereafter sent for Sanger sequencing at a commercial lab (Inqaba Biotechnical Industries (Pty), Ltd., South Africa). The partial 16S rRNA nucleotide sequences obtained were compared to the available nucleotide sequences in the National Centre for Biotechnology Information (NCBI) GenBank database using Basic Local Alignment Search Tool (BLAST). The sequence showing > 97% similarities was selected and used to construct the phylogenetic tree (maximum likelihood) using MEGA 7 software.

Transmission electron microscopy

The thylakoid membranes and PBS arrangement in *Euhalothece* sp. KZN were analysed using transmission electron microscopy (TEM). Preparation for electron microscopy was done according to the method of Loza et al. (2013) with some modification. In brief, samples were transferred to 2% bacteriological agar in 0.1 M phosphate buffer (pH 7.2), following fixation in 3% glutaraldehyde in 0.1 M phosphate buffer (pH 7.2), and incubated for 24 h at 4 °C. Subsequently, the samples were washed using 0.1 M phosphate buffer (pH 7.2) and post-fixed in 1% osmium tetroxide made up in the same buffer for 2 h at 4 °C. Samples were then dehydrated in increasing concentrations of ethanol (30–100% *v*/*v*). Thereafter, were progressively infiltrated the samples then embedded in Spurr's resin and allowed to polymerise at 65 °C for 72 h. Ultrathin sections were cut with an ultramicrotome using glass knives and stained with uranyl acetate and lead citrate. The sections were observed using a JEOL 1010 transmission electron microscope (JEOL, USA) operated at 100 kV.

Experimental setup

The growth medium used in this study was BG11 medium (Stanier et al. 1971). The medium was prepared using filtered (100-μm mesh stainless sieve) seawater (Sigma-Aldrich) and supplemented with ± 90 g L^{-1} of natural sea salt (total salinity 120 g L^{-1}). The salinity of the seawater used to make up the medium was measured using a multiparameter YSI 556 MPS system (Yellow Spring Systems, USA). Screening and optimisation experiments were performed in 250 mL Erlenmeyer flasks with 100 mL medium. The flasks were inoculated with an exponentially growing culture [10% (*v*/*v*)] under previously mentioned cultivation conditions.

Experimental designs

The components of BG11 medium were used in two statistically designed experiments in order to optimise C-PC production. Design-Expert 9.0 software (Stat-Ease, Inc., USA) was used for the experimental design, quadratic model building and analysis of the experimental data (Montogomery 2012).

Fractional factorial design

The purpose of the screening step was to identify the medium components that had a significant effect on C-PC synthesis. Six medium components, i.e. $NaNO_3$, K_2HPO_4, $MgSO_4$, $CaCl_2$, trace metal and minor nutrients at varying concentrations, were evaluated. The selection of the low and high levels for each nutrient is important; therefore, the range of each of the nutrients selected was based on the previous literature (Burrows et al. 2008; Singh et al. 2009; Deshmukh and Puranik 2010; Moraes et al. 2013; Venkata Ramana Reddy et al. 2015). The concentration and levels of the variables utilised are listed in Table 1. C-PC (mg g^{-1}) was selected as the response, which can be calculated using Eq. (1)

$$y = \beta_0 + \sum_{i}^{k} \beta_i X_i + \sum 0 \sum_{i<j} \beta_{ij} x_i x_j + \in \quad (1)$$

where y is the predicted response, β_0 is the intercept of the plane, β_i is the constant coefficient of the equation, x_i and x_j are coded independent factors and ϵ is the random error term. Analysis of variance (ANOVA) (type III) was conducted to test the significance of the model and selected factors as shown in Online Resource 1.

Central composite design

Central composite design is one of the most widely used RSM designs which allows one to evaluate the relationship between independent factors and to predict the response in an effective experimental design (Myers et al. 2009; Montogomery 2012). Based on the results from the FFD analysis, $MgSO_4$, $NaNO_3$ and minor nutrients were found to have a significant effect on C-PC yield and were subsequently selected to determine their individual and combined effects on C-PC yield. A 20-run CCD was used for three independent factors with five levels ($-\alpha$, −1, 0, +1, $+\alpha$), six replicates of the central points and six axial points, leading to a total of 20 sets of experiments. The design matrix indicating the concentration of the three media components with respect to their values in actual and coded form, as well as the actual and predicted values of the C-PC yield, is outlined in Table 2. The results from the previous experiment were used to establish the minimum and maximum ranges. The optimum levels of the selected factors were obtained by solving the regression equation and also by analysing the response surface contour plots. The responses were optimised by the second-order model shown in Eq. (2)

$$y = \beta_0 + \sum_{i=1}^{k} \beta_i X_i + \sum_{i=1}^{k} \beta_{ii} x_i^2 + \sum 0 \sum_{i<j} \beta_{ij} x_i x_j + \in \quad (2)$$

where y is the predicted response; β_0, β_i, β_{ii} and β_{ij} were the intercept, the linear coefficient, the squared coefficient and the interaction coefficients of the model, respectively; k is the number of factors; and x_i and x_j are the level of independent factors in the study. In order to confirm the reliability of the developed RSM model, the predicted results were compared with the experimental values (actual C-PC yield).

Table 1 Detailed experimental design for FF0621 with the coded and actual values of the variables tested indicating low, high and central points as well as actual, predicted and residual values for C-PC production from *Euhalothece* sp. KZN

Run order	(X_1) $NaNO_3$ (g L^{-1})		(X_2) K_2HPO_4 (g L^{-1})		(X_3) $MgSO_4$ (g L^{-1})		(X_4) $CaCl_2$ (g L^{-1})		(X_5) trace metal (mL L^{-1})		(X_6) minor nutrients (mL L^{-1})		Actual PC (mg g^{-1})	Predicted PC (mg g^{-1})	Residual[a]
	Actual level	Coded level	Actual level	Coded level	Actual level	Coded level	Actual level	Coded level	Actual level	Coded level	Actual level	Coded level			
1	0.5	−1	0.06	1	0.10	1	0.06	1	0.50	−1	10.00	1	18.40	19.27	−0.87
2	1.50	1	0.02	−1	0.10	1	0.06	1	0.50	−1	5.00	−1	19.98	20.70	−0.72
3	1.50	1	0.06	1	0.10	1	0.06	1	1.50	1	10.00	1	28.09	28.13	−0.04
4	0.5	−1	0.06	1	0.03	−1	0.04	−1	1.50	1	10.00	1	15.59	15.58	0.01
5	1.00	0	0.04	0	0.07	0	0.05	0	1.00	0	7.50	0	22.83	22.36	0.47
6	2.00	1	0.06	1	0.03	−1	0.04	−1	0.50	−1	10.00	1	25.49	26.41	−0.92
7	1.50	1	0.02	−1	0.03	−1	0.06	1	1.50	1	10.00	1	22.55	22.41	0.14
8	1.50	1	0.02	−1	0.10	1	0.04	−1	0.50	−1	10.00	1	29.40	28.59	0.81
9	0.5	−1	0.06	1	0.10	1	0.04	−1	0.50	−1	5.00	−1	12.77	11.99	0.78
10	0.5	−1	0.02	−1	0.10	1	0.06	1	1.50	1	5.00	−1	14.55	14.73	−0.18
11	0.5	−1	0.02	−1	0.03	−1	0.06	1	0.50	−1	10.00	1	16.51	15.74	0.76
12	1.00	0	0.04	0	0.07	0	0.05	0	1.00	0	7.50	0	21.73	22.36	−0.63
13	1.5	1	0.02	−1	0.03	−1	0.04	−1	1.50	1	5.00	−1	12.22	12.45	−0.23
14	1.00	0	0.04	0	0.07	0	0.05	0	1.00	0	7.50	0	22.66	22.36	0.30
15	0.5	−1	0.06	1	0.03	−1	0.06	1	1.50	1	5.00	−1	10.44	10.36	0.08
16	1.50	1	0.06	1	0.10	1	0.04	−1	1.50	1	5.00	−1	18.29	18.17	0.12
17	0.5	−1	0.02	−1	0.10	1	0.04	−1	1.50	1	10.00	1	20.04	19.95	0.10
18	0.5	−1	0.02	−1	0.03	−1	0.04	−1	0.50	−1	5.00	−1	7.78	8.46	−0.68
19	1.00	0	0.04	0	0.07	0	0.05	0	1.00	0	7.50	0	18.40	22.36	−0.21
20	1.50	1	0.06	1	0.03	−1	0.06	1	0.50	−1	5.00	−1	19.98	18.52	0.83
21	1.00	0	0.04	0	0.07	0	0.05	0	1.00	0	7.50	0	28.09	22.36	0.06

[a] The difference between experimental and predicted results, resolution IV design with 16 runs and 5 central points

C-phycocyanin analysis

Cyanobacterium cells from each flask were harvested by centrifugation at 8000×*g* for 10 min at 4 °C. The pellet was washed with 10 mM sodium phosphate buffer (pH 7.0) and subjected to repeated freeze-thaw cycles of − 20 at 4 °C. The buffer was prepared using ultrapure water (18.2 MΩ-cm) supplemented with sodium azide 0.02% (*w*/*v*). The cell debris was removed by centrifugation at 17,000×*g* for 30 min, and the supernatant layer containing C-PC was collected for further analysis. The concentration of the total crude C-PC was determined at 620 and 650 nm according to Bennett and Bogorad (1973). The C-PC concentration in the sample was calculated using Eq. (3)

$$\text{C-PC}\left(\text{mg mL}^{-1}\right) = \frac{\text{OD}_{620\ \text{nm}} - 0.7 \times \text{OD}_{650\ \text{nm}}}{7.38} \quad (3)$$

The total C-PC (mg g^{-1}) extracted from the biomass was determined using Eq. (4)

$$\text{C-PC}\left(\text{mg mg}^{-1}\right) = \frac{\text{C-PC}\left(\text{mg mL}^{-1}\right) \times \text{Volume (mL)}}{\text{Biomass (g)}} \quad (4)$$

Results

Cyanobacterium identification

The cyanobacterium cells were unicellular and blue-green in colour with a wide oval-to-cylindrical shape approximately 8–10 μm in size (Fig. 1a). Cell division was perpendicular to the longer axis of oval cells. The actively diving cells appeared to be smooth, whereas the older cells had irregular net-like granule appearance and were buoyant. On the basis of morphological features observed using the light microscope, the cyanobacterium belonged to the order Chroococcales (subsection 1). The

Table 2 Central composite design was used for three independent factors with five levels ($-\alpha, -1, 0, +1, +\alpha$) and six replicates of the central points and six axial points, leading to a total of 20 sets of experiments

Run	$NaNO_3$ (g L^{-1})		$MgSO_4$ (g L^{-1})		Minor nutrients: citric acid, EDTA-iron citrate, $CaCl_2$ and Na_2CO_3 (mL L^{-1})		Actual C-PC (mg g^{-1})	Predicted C-PC (mg g^{-1})	Residual[a]
	Coded level	Actual level	Coded level	Actual level	Coded level	Actual level			
1	1.00	− 1	0.12	1	15.00	1	25.58	26.22	− 0.64
2	2.00	1	0.12	1	15.00	1	27.99	27.09	0.90
3	1.50	0	0.08	0	17.56	1.682	23.30	22.62	0.68
4	1.50	0	0.08	0	11.25	0	42.65	42.18	0.47
5	2.00	1	0.12	1	7.50	− 1	42.65	41.34	1.32
6	1.00	− 1	0.12	1	7.50	− 1	27.58	26.98	0.59
7	1.50	0	0.15	1.682	11.25	0	31.88	32.97	− 1.09
8	1.50	0	0.08	0	4.94	− 1.682	25.16	26.44	− 1.27
9	1.50	0	0.08	0	11.25	0	40.93	42.18	− 1.25
10	0.66	− 1.682	0.08	0	11.25	0	30.99	29.94	1.05
11	1.50	0	0.01	− 1.682	11.25	0	14.56	14.06	0.50
12	2.34	1.682	0.08	0	11.25	0	27.02	28.66	− 1.64
13	2.00	1	0.04	− 1	7.50	− 1	17.54	16.48	1.06
14	1.50	0	0.08	0	11.25	0	43.23	42.18	1.05
15	1.00	− 1	0.04	− 1	15.00	1	27.69	28.59	− 0.90
16	1.50	0	0.08	0	11.25	0	39.24	42.18	− 2.94
17	2.00	1	0.04	− 1	15.00	1	12.53	12.71	− 0.17
18	1.50	0	0.08	0	11.25	0	44.73	42.18	2.55
19	1.50	0	0.08	0	11.25	0	42.40	42.18	0.22
20	1.00	− 1	0.04	− 1	7.50	− 1	18.39	18.88	− 0.49

[a] The difference between experimental and predicted results (for this set of experiments, α)

molecular identity of the isolate based on 16S rRNA gene sequencing and BLAST analysis confirmed that the isolate falls within a clade of halophilic cyanobacteria and was found to be closely associated with form genus *Euhalothece* strains, a group that receives strong support (RLS = 100%) (Fig. 1b). Partial 16S rRNA gene sequence of the cyanobacterium was deposited in the NCBI database (accession number KF017202).

Phycobiliproteins and phycobilisomes in *Euhalothece* sp. KZN

The blue-green colour of the cells is due to the major PBP, i.e. C-PC, occurring in the PBS rods. The blue colour and peak of the absorption spectrum at 620 nm confirm the production of C-PC (Fig. 2). In the case of C-PC, denaturation leads to a loss of absorbance at 620 nm (first excited state) and an increase in absorbance at 360 nm (second excited state). The spectra of the extract did not reveal the characteristic PE peak in the range of 565 nm. In Fig. 3, the PBSs are the dense structures lying on the thylakoid membrane of the *Euhalothece* sp. KZN.

Effect of nutrients on C-PC production using fractional factorial design

The initial aim was to determine the effect of individual BG11 nutrient concentrations on C-PC production in *Euhalothece* sp. KZN. Pareto chart illustrates the magnitude of significance of each nutrient affecting C-PC production (Fig. 4). This was estimated as the difference between averages of measurements made at the high level (+ 1) and the low level (− 1) of that factor. Based on the Pareto chart and small p value, minor nutrients (citric acid, ferric ammonium citrate, EDTA and Na_2CO_3), $NaNO_3$ and $MgSO_4$ were identified to have positive impact factors on C-PC production.

The yield of C-PC may be best predicted using Eq. (4)

$$\begin{aligned} Y\left(\text{mg g}^{-1}\right) = {} & 2.57 + 0.50 \times X_1 + 0.06 \times X_2 + 0.25 \times X_3 \\ & + 0.06 \times X_4 + {-}0.06 \times X_5 + 0.52 \times X_6 \\ & + 0.09 \times X_1X_2 + {-}0.1 \times X_1X_5 + 0.08 \times X_1X_6 \\ & + {-}0.07 \times X_2X_6 \end{aligned} \quad (4)$$

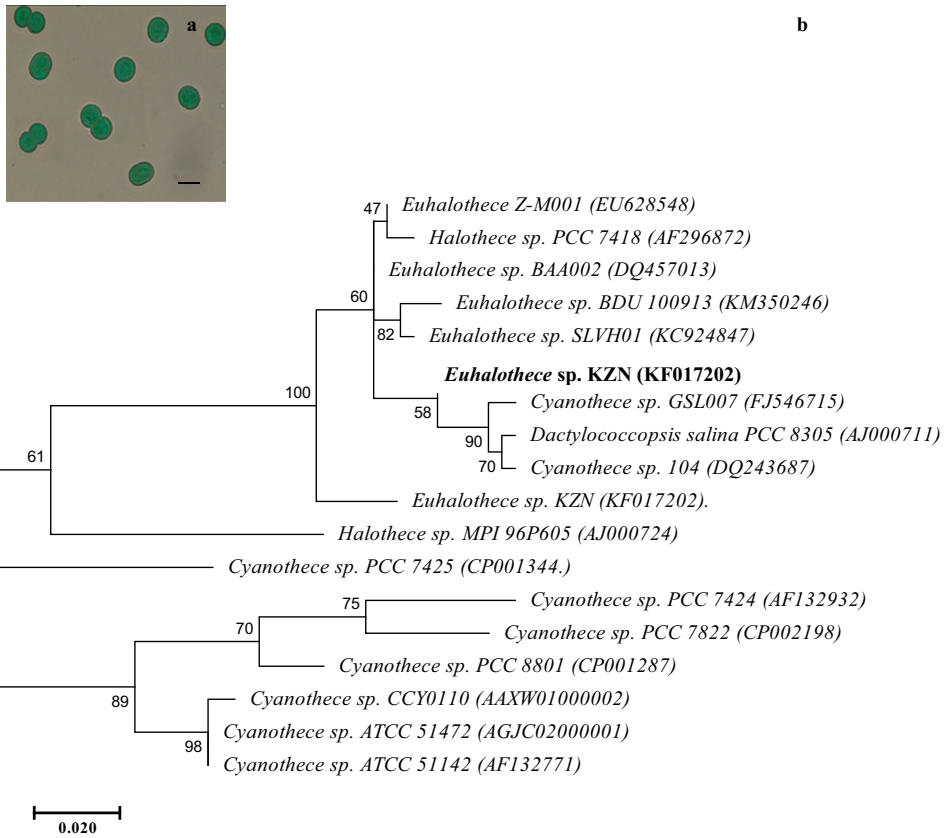

Fig. 1 **a** Micrograph showing blue-green *Euhalothece* sp. KZN cells. **b** Reconstructed phylogenetic tree of *Euhalothece* sp. KZN and related cyanobacteria that were aligned based on 16S rRNA sequences. The Kimura two-parameter model along with 1000 bootstrap replications was selected to construct the maximum likelihood tree. Bootstrap values (distance) of ≥ 50% are indicated on the branches. The bar shows genetic distance. All sequences were extracted from NCBI database (www.ncbi.nlm.nih.gov). Multiple sequence alignments were performed using the BioEdit sequence alignment editor. Sequence alignment as well as tree building were performed using MEGA7

Minor nutrients (citric acid, ferric ammonium citrate, EDTA and Na_2CO_3) showed the highest positive effect on C-PC yield with an F value of 383,630 and a significant p value < 0.0001. The positive effect for minor nutrients suggests that the medium requires a higher level of minor nutrients than optimum to enhance C-PC production. Thus, the minor nutrient solution was selected as the first essential medium component to be optimised. N also showed a positive effect and contributed 19.13% to the total effects of the F and p values of 365.95 and < 0.0001, respectively, showing the significance of N in C-PC production. The significance of $MgSO_4$ in C-PC production is evident from the low p value of 0.0101. Potassium dihydrogen phosphate and $CaCl_2$ were found have a positive but insignificant effect towards C-PC production in terms of the percentage contribution of 1.74 and 2.67, respectively. Increasing the concentration of the inorganic salt KH_2PO_4 did not show any effect on C-PC synthesis in this study. This indicated that 0.06 g L^{-1} in the medium is sufficient for C-PC

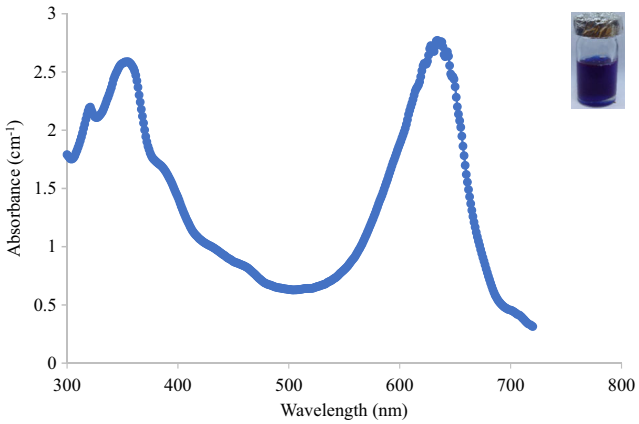

Fig. 2 UV-vis absorbance spectra of crude PBP extract. Inset vividly coloured blue PBPs

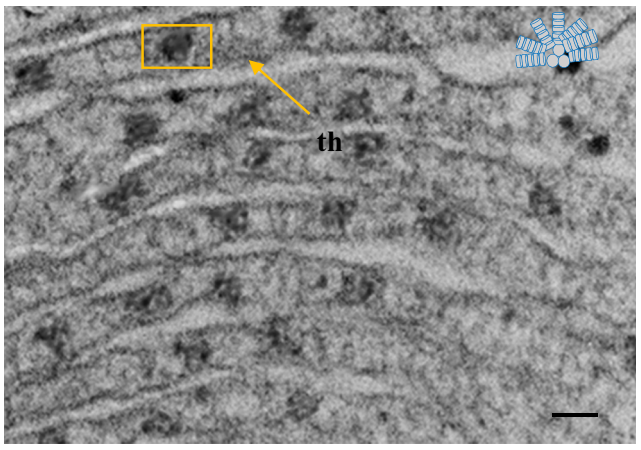

Fig. 3 Transmission electron micrographs of *Euhalothece* sp. KZN cell showing parallel thylakoid membranes (th), and dense structures representing PBS, a schematic drawing of PBS, are also shown. Scales bars are 50 nm

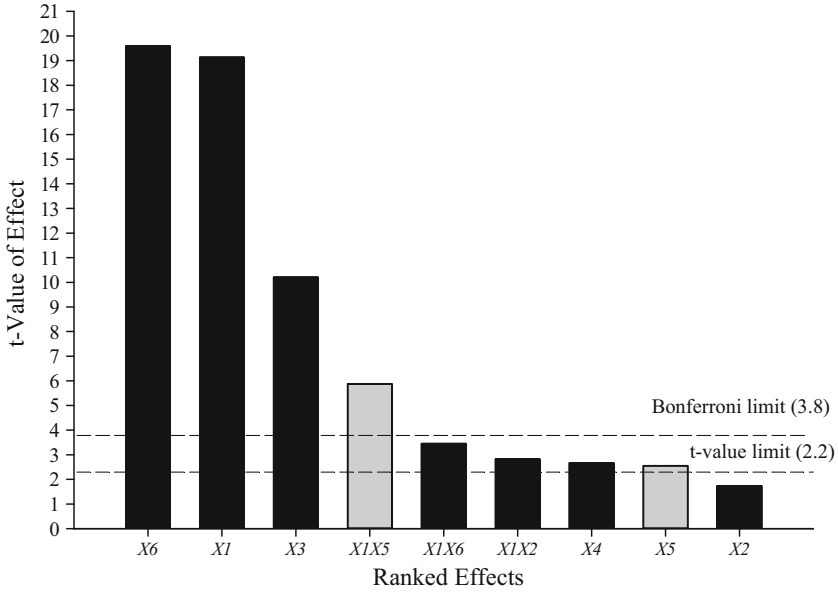

Fig. 4 Pareto chart indicating the magnitude of significance of media components on C-PC production. The individual components minor nutrients (X_6), and NaNO (X_1) and MgSO (X_3) showed significant positive effect, while the interaction between $NaNO_3$ (X_1) and trace metals (X_5) showed negative effect towards CPC production. The other nutrients, K HPO (X) and CaCl (X) had a positive but insignificant effect. Solid black bars indicate positive effects, and white bars indicate negative effects. Bars above the Bonferroni limit (3.8) are certainly significant while those above the t-value limit (2.2) are possibly significant

synthesis in *Euhalothece* sp. KZN. On the contrary, trace metals and the interaction between trace metals and $NaNO_3$ showed negative effects of − 0.12 and − 0.28. Trace metals showed a 2.55% contribution, and the interaction between trace metals and $NaNO_3$ showed 2.88% contribution with an F value of 7.99. This demonstrates that − 1 level (i.e. at low concentration) of trace metals in the medium favoured C-PC production in this cyanobacterium. The above results indicate that the trace metals did not play an active role in the C-PC production.

Optimisation and role of nutrients in C-PC production using response surface methodology

Response surface methodology was used to determine the optimal level of the nutrients as well as to study the interactions amongst the selected media components: $NaNO_3$, $MgSO_4$ and minor nutrients (citric acid, ferric ammonium citrate, EDTA and Na_2CO_3) for enhancing C-PC synthesis in *Euhalothece* sp. KZN. Equation (5) describes the mathematical model relating to the production of C-PC with independent variables and the second-order polynomial through multiple regression analysis using Design-Expert 9.0. The equation provides an estimate of the level of C-PC (Y) as a function of $NaNO_3$ (X_1), $MgSO_4$ (X_3) and minor nutrients (X_6). The response equation from the above set of experiments can be written as

$$Y\left(\text{mg g}^{-1}\right) = 42.18 + 5.62 \times X_3 — 0.38 \times X_1 - 1.14 \times X_6 + 4.19 \times X_3X_1 - 2.62 \times X_3X_6 - 3.37 \times X_6 - 6.60 \times X_3^2 - 4.55 \times X_1^2 - 6.24 \times X_6^2 \quad (5)$$

An ANOVA of the quadratic regression model (Eq. (5)) showed that the model significantly fitted the data, as was evident from the low p value (< 0.0001) of Fisher's test. The results showed that the linear effect of $MgSO_4$ (X_3) and minor nutrients (X_6) as well as the interactive effects of $NaNO_3$ and $MgSO_4$ (X_1X_3), $NaNO_3$ and minor nutrients (X_1X_6) and $MgSO_4$ and minor nutrients (X_3X_6) were also significant model terms. The fit of the model variables was determined by the coefficient of determination (R^2). Based on the ANOVA results (Online Resource 2), the model reported a high R^2 value of 0.9847, indicating that 98.47% of the variability in the responses could be explained by the model. An adjusted R^2 value of 0.9709 was also found, and since they are close to 1.0, this indicates a high correlation between the experimental values and the predicted values. The lack of fit was found to be insignificant (p value = 0.0642) which indicated that the developed model data fitted the variables. Based on above, the actual relationship between the response and the significant variables could be confidently described by the developed model.

The optimum levels of the selected medium components were obtained by analysing the response surface plots. The contour plots described by the regression model were drawn to illustrate the individual and interactive effects of $MgSO_4$, NO_3 and minor nutrient stock (citric acid, ferric ammonium citrate, EDTA and Na_2CO_3) on C-PC production by *Euhalothece* sp. KZN. The response surface plot (Fig. 5a) clearly shows the interaction between NO_3 and minor nutrients. Increasing $NaNO_3$ (1 to 1.8 g L^{-1}) and minor nutrient (7.5 to 10 mL L^{-1}) concentrations in the media led to an overall increase in C-PC yield (42.65 mg g^{-1}). However, a further increase in NO_3 concentration to 2 g L^{-1} led to a decrease in C-PC yield (27.01 mg g^{-1}). The minor nutrients which composed of citric acid, ferric ammonium citrate, EDTA disodium salt and Na_2CO_3 were found to be crucial for stimulating C-PC synthesis.

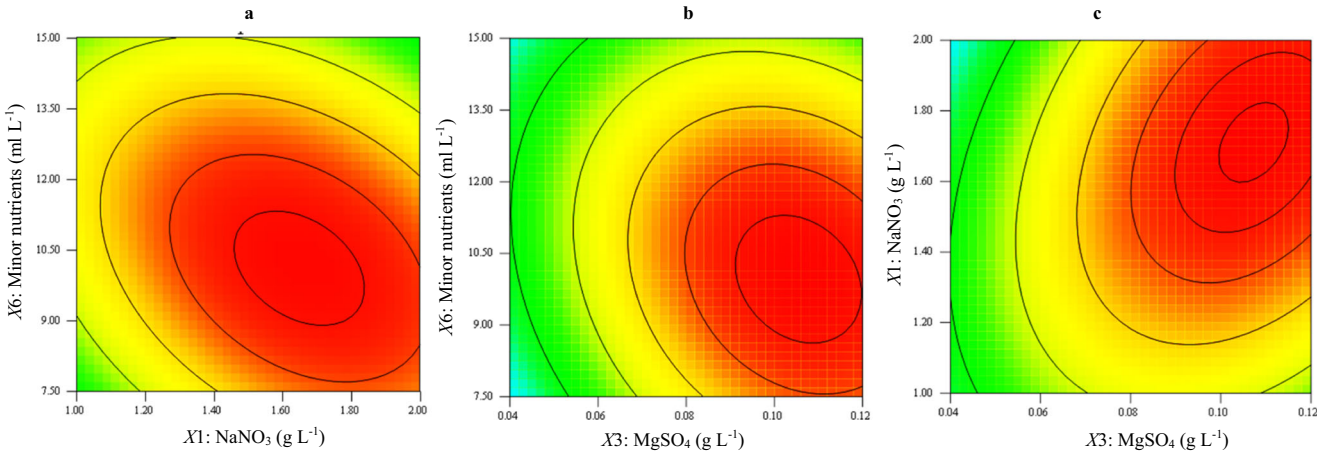

Fig. 5 Response surface contour plots for C-PC production by Euhalothece sp. KZN, showing (a) minor nutrients and MgSO while NaNO was kept at a constant level (1.5 g L-1), (b) minor nutrients and NaNO while MgSO was kept at 0.08g L-1, and (c) MgSO and NaNO while minor nutrients were kept at a constant level (11.25 ml L-1)

Similarly, the C-PC concentration increased proportionally with an increase in $MgSO_4$ and minor nutrients in the medium (Fig. 5b). Increasing $MgSO_4$ concentration from 0.04 to 0.11 g L^{-1} and that of minor nutrients from 7.5 to 10 mL L^{-1} while keeping $NaNO_3$ constant at 1.5 g L^{-1} greatly increased the C-PC yield from 3.82 to 5.62 mg g^{-1}. It is important to note that when the $MgSO_4$ concentration was increased beyond α level (0.15 g L^{-1}), the C-PC yield decreased. The predicted optimum concentrations of minor nutrients and $MgSO_4$ were observed near 10 mL L^{-1} and 0.11 g L^{-1}, respectively. When both nutrient factors were kept at low levels, the C-PC yield was low.

Experimental validation

A confirmatory experiment at different levels of the factors, as suggested by the numerical modelling to support data under optimised conditions, was performed. This experiment was conducted to maximise C-PC content while keeping other responses within the range. On the basis of numerical optimisation, the quadratic model predicted that the maximum C-PC production was a mean of 95% CI of 43.97 ± 1.76 mg g^{-1} when the optimal values of test factors were 0.10 g L^{-1} of $MgSO_4$, 1.67 g L^{-1} of $NaNO_3$ and 10 mL L^{-1} of minor nutrients. The predicted optimum concentration of nutrients was validated at the suggested levels in triplicate. The maximum C-PC obtained under optimum conditions was 45 mg g^{-1}, which was within the 95% CI of the prediction value (Fig. 6). This indicated that the model was precise when predicting the optimal nutrient concentrations for improved C-PC production. Moreover, the use of RSM significantly enhanced the C-PC yield by > 280% in comparison to the un-optimised BG11 medium. Therefore, the applied model was considered to be reliable for predicting the production of C-PC from *Euhalothece* sp. KZN.

Discussion

Cyanobacterium identification

Bergey's manual of systematic bacteriology classifies the cyanobacteria in 'form genera' which, in turn, are divided into clusters or subclusters, but not an 'official classification' (Ramos et al. 2017). Waterbury and Rippka (1989) proposed that the coccoid to rod-shaped cyanobacteria with cells larger than 3 μm in diameter dividing by binary fission in one plane perpendicular to the long axis and lacking a sheath were placed in the provisional *Cyanothece* group. Garcia-Pichel et al. (1998) described the common characteristics of strains belonging to the *Halothece* cluster of the form genus *Cyanothece* are extremely halotolerant with optimal salinities between 5 and 20%, moderate thermophiles, i.e. growth at 45 °C, and only contain C-PC pigment. Marine and freshwater unicellular *Cyanothece* that cannot grow at high NaCl concentration do not cluster within *Halothece*. The results from our analysis (cell shape, size, pigment composition and salt

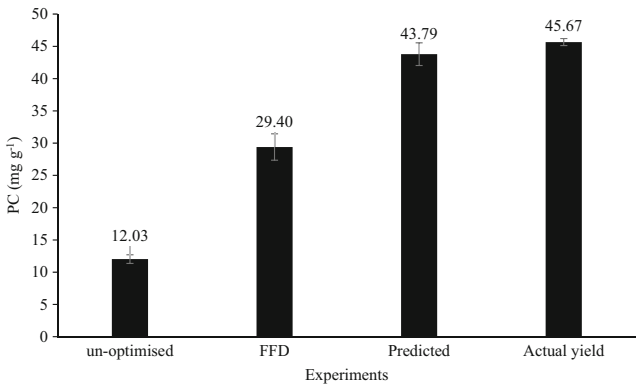

Fig. 6 C-phycocyanin yield obtained in the original and optimised BG11 medium from *Euhalothece* sp. KZN. Error bars represent means ± SEM. $n = 3$

tolerance) indicate the isolated strain-resembled members of the order Chroococcales, genus *Cyanothece*, cluster 3 *Halothece*/*Euhalothece*. Traditionally, cyanobacteria are identified on the basis of their morphological characteristics; however, recently, molecular characterisation is widely used to confirm the identity of cyanobacterial species. The isolated cyanobacterium is closely related cyanobacteria that are associated with extreme conditions. For example, the isolate shared identities (> 96%) to *Euhalothece* sp. Z-M001 isolated from Soda Lake, Magadi (Mikhodiuk et al. 2008); *Dactylococcopsis salina* PCC 8305 isolated from a Solar Lake in Sinai, Egypt (Walsby et al. 1983); *Euhalothece* sp. from the United Arab Emirates (Mckay et al. 2016); and *Cyanothece* sp. 104 isolated from seawater off China's coast (Zhang et al. 2007). Garcia-Pichel et al. (1998) reported *Halothece* PCC 7418 isolated from Solar Lake, Sinai, Egypt, along with 11 other cyanobacterial isolates from solar evaporation and hypersaline ponds. The analysis showed that amongst all the matches for the 16S rRNA gene sequences from GenBank, the isolate showed 100% similarity to *Euhalothece* and *Halothece* genera.

The genus *Halothece* was first created by Garcia-Pichel et al. (1998) following phylogenetic, 16S rRNA gene-based analysis of 13 extremely halotolerant unicellular cyanobacterial strains previously isolated from various hypersaline environments. Two distinct subclusters were described: (1) '*Euhalothece*', comprising 12 closely related strains of similar morphology and were originally identified as members of three traditional genera (*Cyanothece*, *Aphanothece* and '*Dactylococcopsis*' (*Myxobakton*)), and (2) 'true *Halothece*', consisting only a single strain, MPI 96P605. Similarly, using 16S rRNA sequence analysis, Margheri et al. (1999) confirmed 11 new halotolerant strains that formed a monophyletic cluster of previously proposed '*Halothece*' genus. Although the strains belonging to this cluster are supported by a molecular analysis, to date, the form genus *Halothece* has no standing under either the International Code of Nomenclature (ICN) for algae, fungi and plants or the International Code of Nomenclature of Prokaryotes (ICNP) as it has not been validly described (Komárek et al. 2014). Even though *Halothece* is not a validated genus, to date, there are approximately 45 isolates that have been assigned to *Halothece*, subcluster *Euhalothece*.

Phycobiliproteins and phyobilisomes in *Euhalothece* sp. KZN

C-phycocyanin is a water-soluble pigment-bound protein used to capture light energy for photosynthesis that constitutes up to 15% of its dry cell weight when harvested (Hazra and Saha Kesh 2017). This pigment is unique to cyanobacteria and is responsible for the distinctive deep blue colour. The blue colour and prominent peak at 620 nm of the absorption spectrum indicated the presence of mainly C-PC (Fig. 2). Due to low concentrations of C-APC in the cell, its major absorption band (650 nm) is masked by those of C-PC. Transmission electron microscopy was done to examine the thylakoid membrane and PBS. The cytoplasmic surface of the thylakoid membranes is separated by the PBS. Phycobilisomes are hemi-discoidal pigment-bound protein complexes that are attached to the cytoplasmic side of the thylakoid membrane (Chang et al. 2015). The PBSs are composed of a core and clusters of rods made up of short stacks of discs (Li et al. 2004). It is known that PBSs naturally have a rectangular shape and stand upright on the thylakoid membrane in the cell (Yi et al. 2005). The appearance of the PBS in thin-section electron micrographs is dependent upon the plane of sectioning of the samples (Cosner 1978). When the rows of PBS are cut in cross section in a plane perpendicular to the thylakoid surface, the PBSs display an irregular semi-circular outline with the flat side attached to the thylakoid membrane and, therefore, appear in face view (Bryant et al. 1979). The PBSs are seen in edge view standing on the thylakoid surface, when the rows of PBS are either cut in longitudinal section in a plane normal to the thylakoid surface or in tangential section, i.e. when the plane of sectioning is parallel to the thylakoid surface (Bryant et al. 1979). The PBSs appear as electron-dense cords running at an angle to the long axis of the cells. As seen in transverse sections (Fig. 6), PBS appears to be dense structures that are anchored on the thylakoid membrane. Similarly, Porta et al. (2000) found that in *Cyanothece* PCC 8303, the alternative distribution of the PBS between two thylakoids gave the PBS a zipper-like appearance. Distortion of PBS shapes within cells could be caused by close contact with the abundant α-granules which compete for the same stromal space (Gray et al. 1973).

Screening and optimisation of nutrients for C-PC production in *Euhalothece* sp. KZN

The selection of the optimal combination of nutrients is essential to increase C-PC production in cyanobacteria. Statistical design strategies for screening and optimisation allow for quick identification of essential nutrients and interactions between them. Amongst the BG11 nutrients screened, three components, viz. minor nutrients (i.e. citric acid, ferric ammonium citrate-EDTA, Na_2CO_3), $NaNO_3$ and $MgSO_4$, showed a significant effect ($p > 0.005$) on C-PC yield (Fig. 4). Based on the results of the CCD, 10 mL L^{-1} of minor nutrients, 1.67 g L^{-1} of $NaNO_3$ and 0.10 g L^{-1} of $MgSO_4$ were the optimum concentrations required for C-PC production. The maximum C-PC yield was demonstrated by a confirmatory experiment using the optimised medium that the predicted values (43.7 mg g^{-1}) agreed well with the experimental values (45 mg g^{-1}) (Fig. 1). The interaction effects of minor nutrients and $NaNO_3$ on C-PC production are shown in Fig. 5a. As seen, increasing the minor nutrient and $MgSO_4$ concentrations up to the optimum point increased the C-PC yield to a

maximum level. However, the C-PC yield decreased following a further increase in the nutrient levels. Similar observations were also noticed for minor nutrients and $MgSO_4$ (Fig. 5b) and for $MgSO_4$ and $NaNO_3$ (Fig. 5c) on C-PC production by *Euhalothece* sp. KZN. The C-PC pathway is shown in Online Resource 3 (Frankenberg and Lagarias 2003; Wiethaus et al. 2010; Alvey et al. 2011; Aoki et al. 2011; Czarnecki and Grimm 2012).

Although, in this study, minor nutrients are not supplied as separate components, ferric ammonium citrate-EDTA and Na_2CO_3 serve as the sources of the essential minerals required for C-PC synthesis. The key enzymes, ferrochelatase and phycocyanobilin/ferredoxin oxidoreductase (PcyA), are regulated by Fe. Ferrochelatase (which contains two Fe-S clusters) is responsible for the insertion of Fe^{2+} into PIX to form heme in step 5 (Alvey et al. 2011) (Online Resource 3). Thus, the increase in ferrochelatase activity is associated with accumulation of heme. The initial step in the PCB biosynthesis is catalysed by heme oxygenase (HO) where heme serves as both the substrate and cofactor for its degradation (Montellano 2000). Spiller et al. (1982) reported that the level of HO enzyme is a rate-controlling factor in PCB synthesis. Biliverdin IXα produced from heme is further reduced by ferredoxin-dependent PcyA (step 7). Thus, the requirement of high concentration of Fe ions is attributed to its inevitable role as a redox cofactor for PcyA. Moreover, Chakdar and Pabbi (2016) reported that Fe regulates the expression of the PC αβ subunit gene. It is well established that Fe deficiency results in oxidative stress; thus, a significant increase in reactive oxygen species triggers the synthesis antioxidants, which include PCB to act as free radical scavengers (Latifi et al. 2005). Tu et al. (2004) observed that Fe limitation (or removal of chelators) results in the accumulation of chlorophyll precursor, protoporphyrin IX monomethyl ester (Mg-ProtoMe). Even though Fe is not a constructional element in PCBs, it is significantly important, since the PCB synthesis has Fe-dependent steps, and Fe serves as a substrate and cofactor for these essential enzymes (Tooley et al. 2001; Wang et al. 2010).

Cyanobacteria also need C compounds in the form of keto acids (oxaloacetate and 2-oxoglutarate) to produce the macromolecules such as amino acids and apoproteins. A study by Stöckel et al. (2013) showed that the glutamate-utilising enzyme, i.e. GluRS that converts glutamate to glu-tRNA (step 2), revealed higher transcript abundance under elevated C conditions. Furthermore, the reduction in the inorganic carbon source (Na_2CO_3) promotes the arrangement of the PBP complex. Previously, a suitable concentration of Na_2CO_3 was found helpful in enhancing the PBP synthesis (Johnson et al. 2014). Deshmukh and Puranik (2012) reported that $CaCl_2$ and Na_2CO_3 were the most influential nutrients for C-PC in *Synechocystis* sp., producing 23 mg L^{-1} of C-PC when cultivated in 0.058 and 0.115 g L^{-1} of $CaCl_2$ and Na_2CO_3, respectively. Sun et al. (2009b) reported that C and Fe limitation resulted in partial loss of pigment since a lack of these essential compounds produces a protein factor (NblC) that initiates the degradation of C-PC.

Generally, the C-PC yield increases with nitrate concentration up to a critical level; however, at a very high nitrate concentration (2 g L^{-1}), C-PC yield decreases. Therefore, in the present study, the optimal nitrate concentration (1.67 g L^{-1}) predicted was justified. Wakte et al. (2011) reported that nutrients such as NO_3 and Mg are required for growth, metabolism as well as the structural and functional components of nucleic acids, proteins and cell wall. Nitrogen accounts for approximately 10% of dry weight, and it is very essential for synthesis of the amino acids which constitute proteins and other cellular compounds including the C-PC subunits of the cyanobacteria (Herrero et al. 1990; Flores and Herrero 1994). Nitrate is actively taken up by cyanobacterial cells and is sequentially reduced by nitrate reductase to nitrite and then to ammonium by nitrite reductase (Liotenberg et al. 1996). Nitrogen assimilation operates through the glutamine synthetase (GS)/glutamate synthase (GOGAT) pathway, which allows incorporation of N to glutamate and glutamine (step 1). Glutamate is a vital precursor for aminolevulinic acid (ALA), the immediate precursor for PCB synthesis (Online Resource 3). Tandeau de Marsac and Houmard (1993) reported that PBP synthesis depends on the supply of assimilable N. The chemical structure of phycobilin consists of four pyrrole rings, where the N atoms form a strong bond between the Fe^{+} ions. At a low nitrate concentration (1 g L^{-1}), C-PC biosynthesis is also low, since an insufficient amount of assimilable N is present in the medium. Lack of N represses the synthesis of new C-PC by suppressing the de novo synthesis of the αβ apoprotein subunits (Xie et al. 2015). It is known that PBPs play a role as N reservoirs; thus, during N limitations, cyanobacteria degrade the PBS and linker proteins to release essential amino acids to synthesise other proteins required to support the metabolic activity of the cells (Richaud et al. 2001). Researchers also have reported that during N and S limitation, the PBP content and the level of C-PC mRNA decrease (Singh et al. 2003; Eisenhut et al. 2007; Ludwig and Bryant 2012). It has also been previously reported that a higher level of nitrate results in an increase in the amount of Fe absorbed by cells (Schwarz and Forchhammer 2005; Leu et al. 2013; Esen and Ozturk Urek 2015). However, a further increase in NO_3 concentration to 2 g L^{-1} led to a decrease in C-PC yield. Comparably, Johnson et al. (2014) reported the synthesis of PBP decreased at a very high concentration of $NaNO_3$ due to an inhibition of PBP biosynthetic enzymes in the presence of excess N.

Similarly, Mg also plays a crucial role in C-PC synthesis, and it is primarily used as a cofactor for porphobilinogen (PBG) synthase enzyme. The formation of ð-ALA is the first committed and rate-limiting step in the synthesis of

phycobilins requiring Mg^{2+}. In cyanobacteria, ALA is normally synthesised from glutamate via the C5 pathway seen in step 3 (Online Resource 3) (Shoolingin-Jordan et al. 2002; Chow 2012; Esen and Ozturk Urek 2015). The PBG synthase enzyme catalyses the condensation of two molecules of ALA with the addition of Mg^{2+} to form the pyrrole ring of PBG (Frankenberg and Lagarias 2003). However, as described previously, excess Mg will be incorporated into the protoporphyrin molecule, to synthesise chlorophyll (Beale 1999), thus decreasing C-PC. Metal ions are often found in the active site of PBGS and are commonly required for enzymatic activity. Jaffee (2003) reported that cyanobacteria, *Synechococcus* sp. and *Synechocystis* sp. which are distantly related to *Euhalothece* sp., have aspartate-rich and allosteric Mg metal binding region, respectively, thus requiring Mg (Jaffee 2003). An increase in Mg concentration up to 0.11 g L^{-1} resulted in an increase in C-PC yield. This finding is in agreement with Wakte et al. (2011) where they have reported the essentiality and significant influence of $MgSO_4$ on C-PC production in *Spirulina* sp.

Conclusions

This study successfully identified and optimised the most critical nutrients required for C-PC production of *Euhalothece* sp. KZN using a strategy of selection and modelling. The optimised strategy could reduce the production cost of C-PC, thus enhancing the feasibility of commercial application of this versatile pigment. The optimum media components for producing maximum C-PC (45 mg g^{-1}) in *Euhalothece* sp. KZN were found to be $MgSO_4$ (0.10 g L^{-1}), $NaNO_3$ (1.67 g L^{-1}) and minor nutrients (10 mL L^{-1}). The outcome of this study resulted in an in-depth understanding of the roles these nutrients play in increasing the C-PC yield, as well as an integrated strategy for enhancing the C-PC in *Euhalothece* sp. KZN.

Acknowledgements We thank our colleagues at the Institute for Water and Wastewater Technology (IWWT), Durban University of Technology (DUT), for their support and guidance.

Funding information This work was supported by the grant from the National Research Foundation, for which the authors are thankful.

References

Allen MM, Stanier RY (1968) Growth and division of some unicellular blue-green algae. J Gen Microbiol 51:199–202

Alvey RM, Biswas A, Schluchter WM, Bryant DA (2011) Effects of modified phycobilin biosynthesis in the cyanobacterium *Synechococcus* sp. strain PCC 7002. J Bacteriol 193:1663–1671

Aoki R, Goto T, Fujita Y (2011) A heme oxygenase isoform is essential for aerobic growth in the cyanobacterium *Synechocystis* sp. PCC 6803: modes of differential operation of two isoforms/enzymes to adapt to low oxygen environments in cyanobacteria. Plant Cell Physiol 52:1744–1756

Bandyopadhyay A, Elvitigala T, Welsh E, Stockel J, Liberton M, Min H, Sherman LA, Pakrasi HB (2011) Novel metabolic attributes of the genus cyanothece, comprising a group of unicellular nitrogen-fixing *Cyanothece*. mBio 2(5). https://doi.org/10.1128/mBio.00214-11

Beale SI (1999) Enzymes of chlorophyll biosynthesis. Photosynth Res 60:43–73

Bennett A, Bogorad L (1973) Complementary chromatic adaptation in a filamentous blue-green alga. J Cell Biol 58:419–435

Bryant DA, Guglielmi G, de Marsac NT, Castets A-M, Cohen-Bazire G (1979) The structure of cyanobacterial phycobilisomes: a model. Arch Microbiol 123:113–127

Burrows E, Chaplen F, Ely R (2008) Optimization of media nutrient composition for increased photofermentative hydrogen production by *Synechocystis* sp. PCC 6803. Int J Hydrog Energy 33:6092–6099

Chakdar H, Pabbi S (2016) Cyanobacterial phycobilins: production, purification, and regulation. In: Shukla P (ed) Frontier discoveries and innovations in interdisciplinary microbiology. Springer India, New Delhi, pp 45–69

Chaneva G, Furnadzhieva S, Minkova K, Lukavsky J (2007) Effect of light and temperature on the cyanobacterium *Arthronema africanum*—a prospective phycobiliprotein-producing strain. J Appl Phycol 19:537–544

Chang L, Liu X, Li Y, Liu CC, Yang F, Zhao J, Sui SF (2015) Structural organization of an intact phycobilisome and its association with photosystem II. Cell Res 25:726–737

Chow F (2012) Nitrate assimilation: the role of in vitro nitrate reductase assay as nutritional predictor. In: Najafpour M (ed) Applied photosynthesis, vol 6. InTech, Rijeka, pp 726–737

Cosner JC (1978) Phycobilisomes in spheroplasts of *Anacystis nidulans*. J Bacteriol 135:1137–1140

Czarnecki O, Grimm B (2012) Post-translational control of tetrapyrrole biosynthesis in plants, algae, and cyanobacteria. J Exp Bot 63:1675–1687

Deshmukh DV, Puranik PR (2010) Application of Plackett-Burman design to evaluate media components affecting antibacterial activity of alkaliphilic cyanobacteria isolated from Lonar Lake. Turk J Biochem 35:114–120

Deshmukh DV, Puranik PR (2012) Statistical evaluation of nutritional components impacting phycocyanin production in *Synechocystis* sp. Braz J Microbiol 43:348–355

Eisenhut M, Aguirre von Wobeser E, Jonas L, Schubert H, Ibelings BW, Bauwe H, Matthijs HC, Hagemann M (2007) Long-term response toward inorganic carbon limitation in wild type and glycolate turnover mutants of the cyanobacterium *Synechocystis* sp. strain PCC 6803. Plant Physiol 144:1946–1959

Eriksen NT (2008) Production of phycocyanin—a pigment with applications in biology, biotechnology, foods and medicine. Appl Microbiol Biotechnol 80:1–14

Esen M, Ozturk Urek R (2015) Ammonium nitrate and iron nutrition effects on some nitrogen assimilation enzymes and metabolites in *Spirulina platensis*. Biotechnol Appl Biochem:62275–62286

Flores E, Herrero A (1994) Assimilatory nitrogen metabolism and its regulation. In: Bryant DA (ed) The molecular biology of cyanobacteria. Kluwer Academic, Dordrecht, pp 487–517

Frankenberg N, Lagarias JC (2003) Phycocyanobilin:ferredoxin oxidoreductase of *Anabaena* sp. PCC 7120. Biochemical and spectroscopic. J Biol Chem 278:9219–9226

Garcia-Pichel F, Nubel U, Muyzer G (1998) The phylogeny of unicellular, extremely halotolerant cyanobacteria. Arch Microbiol 169:469–482

Glazer AN (1994) Phycobiliproteins—a family of valuable, widely used fluorophores. J Appl Phycol 6:105–112

Gray BH, Lipschultz CA, Gantt E (1973) Phycobilisomes from a blue-green alga *Nostoc* species. J Bacteriol 116:471–478

Hazra P, Saha Kesh G (2017) Isolation and purification of phycocyanin from cyanobacteria of a mangrove forest. Appl Biol Chem 60:631–636

Herrero A, Vega-Palas MA, Martín-Nieto J, Muro-Pastor AM, Madueño F, Flores E (1990) Molecular biology of the assimilation of nitrogenous compounds by cyanobacteria. In: Ullrich R, Rigano C, Figgi A, Aparicio PJ (eds) Inorganic nitrogen in plants and microorganisms. Springer, Berlin, pp 308–311

Hong S-J, Lee C-G (2008) Statistical optimization of culture media for production of phycobiliprotein by *Synechocystis* sp. PCC 6701. Biotechnol Bioprocess Eng 13:491–498

Jaffee EK (2003) An unusual phylogenetic variation in the metal ion binding sites of porphobilinogen synthase. Chem Biol 10:25–34

Johnson EM, Kumar K, Das D (2014) Physicochemical parameters optimization, and purification of phycobiliproteins from the isolated *Nostoc* sp. Bioresour Technol 166:541–547

Kannaujiya VK, Sundaram S, Sinha RP (2017) Phycobiliproteins: recent developments and future applications. Springer, Singapore

Kaushal S, Singh Y, Khattar JIS, Singh DP (2017) Phycobiliprotein production by a novel cold desert cyanobacterium *Nodularia sphaerocarpa* PUPCCC 420.1. J Appl Phycol 29:1819–1827

Kenekar AA, Deodhar MA (2013) Effect of varying physicochemical parameters on the productivity and phycobiliprotein content of indigenous isolate *Geitlerinema sulphureum*. Biotechnol Bioprocess Eng 12:146–154

Komárek J (2016) A polyphasic approach for the taxonomy of cyanobacteria: principles and applications. Eur J Phycol 51:346–353

Komárek J, Kaštovsky′ J, Mareš J, Johansen JR (2014) Taxonomic classification of cyanoprokaryotes (cyanobacterial genera) using a polyphasic approach. Preslia 86:295–335

Kuddus M, Singh P, Thomas G, Al-Hazimi A (2013) Recent developments in production and biotechnological applications of C-phycocyanin. Biomed Res Int. https://doi.org/10.1155/2013/742859

Latifi A, Jeanjean R, Lemeille S, Havaux M, Zhang CC (2005) Iron starvation leads to oxidative stress in *Anabaena* sp. strain PCC 7120. J Bacteriol 187:6596–6598

Leu J-Y, Lin T-H, Selvamani MJP, Chen H-C, Liang J-Z, Pan K-M (2013) Characterization of a novel thermophilic cyanobacterial strain from Taian hot springs in Taiwan for high CO_2 mitigation and C-phycocyanin extraction. Process Biochem 48:41–48

Li D-H, Yang S-Z, Li H, Xie J, Zhao J-Q (2004) Monolayer film of phycobilisome-thylakoid membrane complexes from *Spirulina platensis*. Photosynthetica 42:365–370

Liotenberg S, Campbell D, Rippka R, Houmard J, Marsac NT (1996) Effect of the nitrogen source on phycobiliprotein synthesis and cell reserves in a chromatically adapting filamentous cyanobacterium. Microbiology 142:611–622

Loza V, Perona E, Carmona J, Mateo P (2013) Phenotypic and genotypic characteristics of Phormidium-like cyanobacteria inhabiting microbial mats are correlated with the trophic status of running waters. Eur J Phycol 48:35–252

Ludwig M, Bryant DA (2012) Acclimation of the global transcriptome of the cyanobacterium *Synechococcus* sp. strain PCC 7002 to nutrient limitations and different nitrogen sources. Front Microbiol 3:1–15

Manirafasha E, Ndikubwimana T, Zeng X, Lu Y, Jing K (2016) Phycobiliprotein: potential microalgae derived pharmaceutical and biological reagent. Biochem Eng J 109:282–296

Margheri MC, Bosco M, Giovannetti L, Ventura S (1999) Assessment of the genetic diversity of halotolerant coccoid cyanobacteria using amplified 16S rDNA restriction analysis. FEMS Microbiol Lett 177(1): 9–16

McKay CP, Rask JC, Detweiler AM, Bebout BM, Everroad RC, Lee JZ, Chanton JP, Mayer MH, Caraballo AA, Kapil B, Al-Awar M, Al-Farraj A (2016) An unusual inverted saline microbial mat community in an interdune sabkha in the rub' al khali (the empty quarter), United Arab Emirates. PloS one 11(3):e0150342. https://doi.org/10.1371/journal.pone.0150342

Mikhodiuk OS, Gerasimenko LM, Akimov VN, Ivanovskii RN, Zavarzin GA (2008) Ecophysiology and polymorphism of the unicellular extremely natronophilic cyanobacterium *Euhalothece* sp. Z-M001 from Lake Magadi. Mikrobiologiia 77:805–813

Montellano PR (2000) The mechanism of heme oxygenase. Curr Opin Chem Biol 4:221–227

Montogomery DC (2012) Design and analysis of experiments, 8th edn. Willey, New York

Moraes IO, Arruda ROM, Maresca NR, Antunes AO, Moraes RO (2013) *Spirulina platensis*: process optimization to obtain biomass. J Food Sci Technol 33:179–183

Myers RH, Montgomery DC, Anderson-Cook C (2009) Response surface methodology: process and product optimization using designed experiment, 8th edn. Wiley, Hoboken

Nübel U, Garcia-Pichel F, Muyzer G (1997) PCR primers to amplify 16S rRNA genes from cyanobacteria. Appl Environ Microbiol 63:3327–3332

Pandey U, Pandey J (2008) Enhanced production of biomass, pigments and antioxidant capacity of a nutritionally important cyanobacterium *Nostochopsis lobatus*. Bioresour Technol 99:4520–4523

Patel A, Mishra S, Pawar R, Ghosh PK (2005) Purification and characterization of C-phycocyanin from cyanobacterial species of marine and freshwater habitat. Protein Expr Purif 40:248–255

Porta D, Rippka R, Hernández-Mariné M (2000) Unusual ultrastructural features in three strains of *Cyanothece* (cyanobacteria). Arch Microbiol 173:154–163

Prasanna R, Pabby A, Saxena S, Singh PK (2004) Modulation of pigment profiles of *Calothrix elenkenii* in response to environmental changes. J Plant Physiol 161:1125–1132

Ramos V, Morais J, Vasconcelos VM (2017) A curated database of cyanobacterial strains relevant for modern taxonomy and phylogenetic studies. Sci Data 4:170054

Richaud C, Zabulon G, Joder A, Thomas J-C (2001) Nitrogen or sulfur starvation differentially affects phycobilisome degradation and expression of the nblA gene in *Synechocystis* strain PCC 6803. J Bacteriol 183:2989–2994

Rippka R, Deruelles J, Waterbury JB, Herdman M, Stanier RY (1979) Generic assignments, strain histories and properties of pure cultures of cyanobacteria. J Gen Microbiol 111:1–61

Rodríguez-Sánchez R, Ortiz-Butrón R, Blas-Valdivia V, Hernández-García A, Cano-Europa E (2012) Phycobiliproteins or C-phycocyanin of *Arthrospira* (*Spirulina*) *maxima* protect against HgCl2-caused oxidative stress and renal damage. Food Chem 135: 2359–2365

Schwarz R, Forchhammer K (2005) Acclimation of unicellular cyanobacteria to macronutrient deficiency: emergence of a complex network of cellular responses. Microbiology 151:2503–2514

Sekar S, Chandramohan M (2008) Phycobiliproteins as a commodity: trends in applied research, patents and commercialization. J Appl Phycol 20:113–136

Shoolingin-Jordan PM, Spencer P, Sarwar M, Erskine PE, Cheung KM, Cooper JB, Norton EB (2002) 5-Aminolaevulinic acid dehydratase: metals, mutants and mechanism. Biochem Soc Trans 30:584–590

Singh AK, McIntyre LM, Sherman LA (2003) Microarray analysis of the genome-wide response to iron deficiency and iron reconstitution in the cyanobacterium *Synechocystis* sp. PCC 6803. Plant Physiol 132: 1825–1839

Singh NK, Parmar A, Madamwar D (2009) Optimization of medium components for increased production of C-phycocyanin from *Phormidium ceylanicum* and its purification by single step process. Bioresour Technol 100:1663–1669

Singh NK, Parmar A, Sonani RR, Madamwar D (2012) Isolation, identification and characterization of novel thermotolerant *Oscillatoria*

sp. N9DM: change in pigmentation profile in response to temperature. Process Biochem 47:2472–2479

Spiller SC, Castelfranco AM, Castelfranco PA (1982) Effects of iron and oxygen on chlorophyll biosynthesis: I. *In vivo* observations on iron and oxygen-deficient plants. Plant Physiol 69:107–111

Stanier RY, Kunisawa R, Mandel M, Cohen-Bazire G (1971) Purification and properties of unicellular blue-green algae (order Chroococcales). Bacteriol Rev 35:171–205

Stöckel J, Elvitigala TR, Liberton M, Pakrasi HB (2013) Carbon availability affects diurnally controlled processes and cell morphology of *Cyanothece* 51142. PLoS One 8(2):e56887

Sun L, Wang S, Gong X, Zhao M, Fu X, Wang L (2009a) Isolation, purification and characteristics of R-phycoerythrin from a marine macroalga *Heterosiphonia japonica*. Protein Expr Purif 64:146–154

Sun L, Wang S, Zhao M, Fu X (2009b) Phycobilisomes from cyanobacteria. Handbook on cyanobacteria: biochemistry, biotechnology and applications. Nova Science Publishers, Inc, New York

Tandeau de Marsac N, Houmard J (1993) Adaptation of cyanobacteria to environmental stimuli: new steps towards molecular mechanisms. FEMS Microbiol Lett 104:119–189

Tooley AJ, Cai YA, Glazer AN (2001) Biosynthesis of a fluorescent cyanobacterial C-phycocyanin holo-alpha subunit in a heterologous host. Proc Natl Acad Sci U S A 98:10560–10565

Tu SL, Gunn A, Toney MD, Britt RD, Lagarias JC (2004) Biliverdin reduction by cyanobacterial phycocyanobilin:ferredoxin oxidoreductase (PcyA) proceeds via linear tetrapyrrole radical intermediates. J Am Chem Soc 126:8682–8693

Venkata Ramana Reddy MB, Lakshmana Rao SS, Rao CS (2015) Optimization of process parameters and media components to increase the biomass of cyanobacteria (blue-green algae) *Anabaena ambigua* using response surface methodology. Asian J Microbiol Biotechnol Environ Sci 17:215–225

Wakte PS, Mohite YS, Bhusare DU (2011) Influence of metal ions on growth and C-phycocyanin production in *Arthrospira* (*Spirulina*) *platensis*. Recent Res Sci Technol 3(5):104–108

Walsby AE, Rijn JV, Cohen Y (1983) The biology of a new gas-vacuolate cyanobacterium, *Dactylococcopsis salina* sp.nov., in Solar Lake. Proc R Soc Lond B 217:417–447

Wang C, Kong HN, Wang XZ, Wu HD, Lin Y, He SB (2010) Effects of iron on growth and intracellular chemical contents of *Microcystis aeruginosa*. Biomed Environ Sci 23:48–52

Waterbury JB, Rippka R (1989) Subsection I. Order Chlorococcales Wettstein 1924, emend. Rippka et al. 1979. In: Staley JT, Bryant MP, Pfennig N, Holt JG (eds) Bergey's manual of systematic bacteriology, vol 3. Williams and Wilkins, Baltimore, pp 1728–1746

Waterbury JB, Stanier RY (1981) Isolation and growth of cyanobacteria from marine and hypersaline environments. In: Starr MP, Stolp H, Trüper HG, Balows A, Schlegel HG (eds) The prokaryotes: a handbook on habitats, isolation, and identification of bacteria. Springer, Berlin, pp 221–223

Wiethaus J, Busch AWU, Dammeyer T, Frankenberg-Dinkel N (2010) Phycobiliproteins in Prochlorococcus marinus: biosynthesis of pigments and their assembly into proteins. Eur J Cell Biol 89:1005–1010

Xie Y, Jin Y, Zeng X, Chen J, Lu Y, Jing K (2015) Fed-batch strategy for enhancing cell growth and C-phycocyanin production of *Arthrospira* (*Spirulina*) *platensis* under phototrophic cultivation. Bioresour Technol 180:281–287

Yi Z-W, Huang H, Kuang T-Y, Sui S-F (2005) Three-dimensional architecture of phycobilisomes from *Nostoc flagelliforme* revealed by single particle electron microscopy. FEBS Lett 579:3569–3573

Zhang Y, Chi Z, Lu W (2007) Exopolysaccharide production by four cyanobacterial isolates and preliminary identification of these isolates. J Ocean Univ China 6:147–152